fluids

MDPI

Article

Valveless Pumping with an Unsteady Stenosis in an Open Tank Configuration

Christos Manopoulos [1] and Dimitrios Mathioulakis [2,*]

[1] Laboratory of Biofluid Mechanics & Biomedical Technology, School of Mechanical Engineering, National Technical University of Athens, 15780 Athens, Greece; manopoul@fluid.mech.ntua.gr
[2] School of Mechanical Engineering, Bahrain Polytechnic, Isa Town P.O. Box 33349, Bahrain
* Correspondence: dimitrios.mathioulakis@polytechnic.bh or mathew@fluid.mech.ntua.gr

Abstract: This work examines the beneficial role of an unsteady stenosis, not driven by any external energy source, as a means for augmenting the flow rate of a valveless pump in a hydraulic loop, including an open tank. In contrast to our previous work, in which the concept of the latter stenosis was introduced for the first time in a horizontal closed loop, here, gravity was taken into account. The stenosis neck cross-sectional area was controlled by the fluid pressure and the opposing force applied externally by a spring of adjustable tension. A pincher compressed and decompressed a part of the pump's flexible tube periodically, with frequencies from 5 Hz to 11 Hz and compression ratios A_b from 24% to 65%. The presence of the stenosis increased the net flow rate by 19 times for A_b = 24% and 6.3 times for A_b = 38%; whereas for A_b = 65%, the flow rates were comparable. The volumetric efficiency varied from 30% to 40% under the presence of the stenosis, and from 2% to 20% without the stenosis. The role of the stenosis was to cause a unidirectional flow, opening during tube compression and closing during decompression. The pressure amplitudes along the flexible tube increased towards the rigid–flexible tube junction (as a result of the wave reflections), which were found to be significantly attenuated by the presence of the stenosis, whereas the flow rate pulsations did not exceed 10% of the mean at the peak net flow rates.

Keywords: valveless pump; unsteady stenosis; flow rate augmentation; wave reflection

Citation: Manopoulos, C.; Mathioulakis, D. Valveless Pumping with an Unsteady Stenosis in an Open Tank Configuration. *Fluids* **2024**, *9*, 141. https://doi.org/10.3390/fluids9060141

Academic Editor: Ivette Rodríguez

Received: 13 May 2024
Revised: 29 May 2024
Accepted: 11 June 2024
Published: 12 June 2024

1. Introduction

The concept of valveless pumping was introduced in the late 19th century [1]. Since then, a lot of research has been undertaken in an effort to find answers to relevant scientific questions and technological issues. The advantage of this type of pump is its simple geometrical features, mainly consisting of a flexible tube or a membrane periodically compressed by a pincher, thus reducing its maintenance cost and increasing its lifetime. Valveless pumps are used in various applications, like drug delivery, dosing chemicals, fuel delivery, etc. Their simple geometry allows for the fabrication of micron-sized valveless pumps of various designs, efficiencies, flow rates, and frequencies of operation. However, a major issue, in general, is their small net flow rates. Elevated flow rates and volumetric efficiencies appear only when the pump's pinching frequencies are close to the resonant frequencies of the hydraulic loop, provided that the pincher is asymmetrically positioned in the loop [2,3]. Since the reciprocating pinching mechanism of this type of pump causes a periodic flow with an alternating sign, an asymmetry within the pinching period can cause, on average, a unidirectional flow. Therefore, there has been a lot of effort on the part of the scientific community to increase the pump's net flow rate by introducing several devices as flow rectifiers. In this respect, tapered tube segments of a fixed geometry are normally used, with the hydraulic losses being higher when the flow is directed towards the divergent part of the tube, owing to flow separation, than when the flow is directed towards the convergent part [4]. In [5], a so-called vortex fluid diode was experimentally examined as a

flow rectifier, and it was found, under steady-flow conditions, to reach a diodicity (i.e., the ratio of reverse to forward hydraulic losses) close to 2 for Re greater than 3000. A similar diodicity was found at much lower Re (Re = 36) in a Tesla micro valve [6]; whereas in [7], it was shown that the performance of the latter valve is superior under pulsating flow conditions. In an extensive review [8] regarding reciprocating displacement micropumps, several ideas are presented as flow rectifying devices, like active valves actuated by various types of drivers such as bimetallic, electrostatic, piezoelectric, pneumatic, and passive check and flap valves. More specifically, attempts to improve the piezoelectric valveless pump are detailed in a review paper [9]. In [10], multiple pinchers are proposed with a phase difference between them to increase the net flow rate; however, it has the characteristics of a peristaltic pump rather than a valveless pump. In [11], the performance of an innovative soft-robotic pincher is compared to a mechanical one, showing the advantages of the first.

The prediction of the velocity and pressure field of a valveless pump is not an easy task, mainly due to the flow unsteadiness imposed by the reciprocating pincher, the complex interaction of the fluid with the flexible tube walls, and the reflections of the pressure and flow rate waves at the flexible–rigid junctions of the hydraulic installation. Especially when the tube is deeply occluded by the pincher, a numerical approach is not feasible due to singularities appearing at locations where the grid cells come into contact. Moreover, the pump net flow rate is a complex function of the pinching frequency, for which no analytic solution is yet available.

In a previous work of the present group [12], a new concept was introduced, which caused a significant flow rate increase in a valveless pump: a very small length of the flexible tube of the pump was periodically squeezed by a spring, causing a local stenosis, the opening of which was time-dependent, varying according to the local time-dependent fluid pressure and the tension of the spring. It has to be stressed that the stenosis opening/closing does not require any external energy source, operating, as it does, as a passive valve. The present work was undertaken in the context of further exploring the efficiency of the latter device. In contrast to the previous configuration of a horizontal closed loop, here, the valveless pump is connected to a loop with an open tank at a height above the pump pincher. The beneficial role of the unsteady stenosis is experimentally verified in this loop configuration, especially when the tube compression ratio takes low values (below 50%), increasing the net flow rate many times compared to the no-stenosis case.

2. Materials and Methods

A hydraulic loop was used, including a 920 mm long flexible tube with an internal diameter D = 12 mm, 1 mm thick, connected to two stiff transparent plastic tubes, each 1300 mm long, of the same internal diameter. Each of the stiff tubes was connected to a water tank (the tanks being side by side; see Figure 1a) at a certain height level above a table on which the pincher of the valveless pump was located with the novel unsteady stenosis device. The latter device includes a compression spring connected, at one side, to a hemi-cylindrical piece of Ertalon, which is always in contact with the flexible tube of the pump, and at the other side, to a regulating screw for adjusting the pretension of the spring. More details of this device are presented in our previous work [12] (see Figure 2). The flowing medium was salt water (10% salt concentration by weight) at an average temperature of 22 °C, which is necessary for the operation of an electromagnetic flow meter.

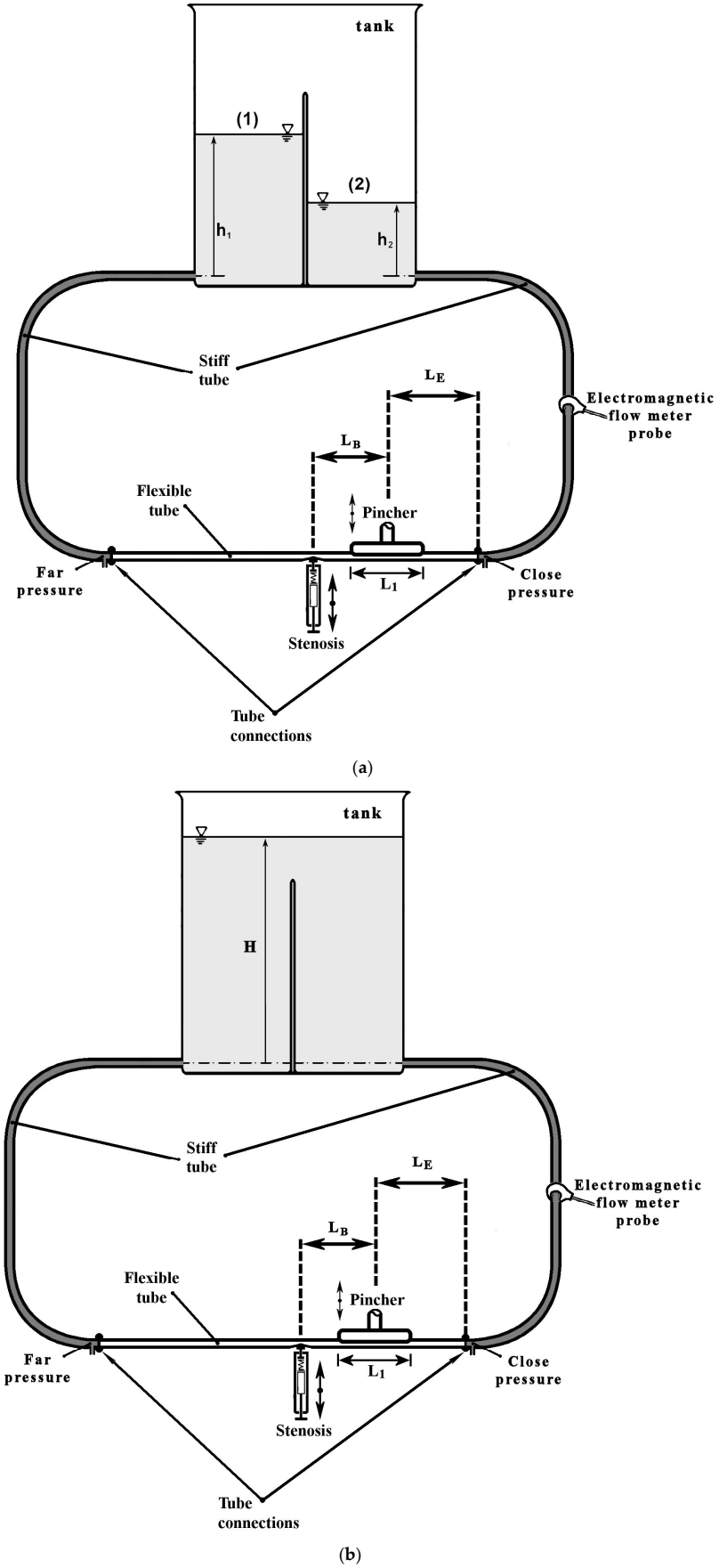

Figure 1. Hydraulic loop: (**a**) two-tank and (**b**) one-tank configuration.

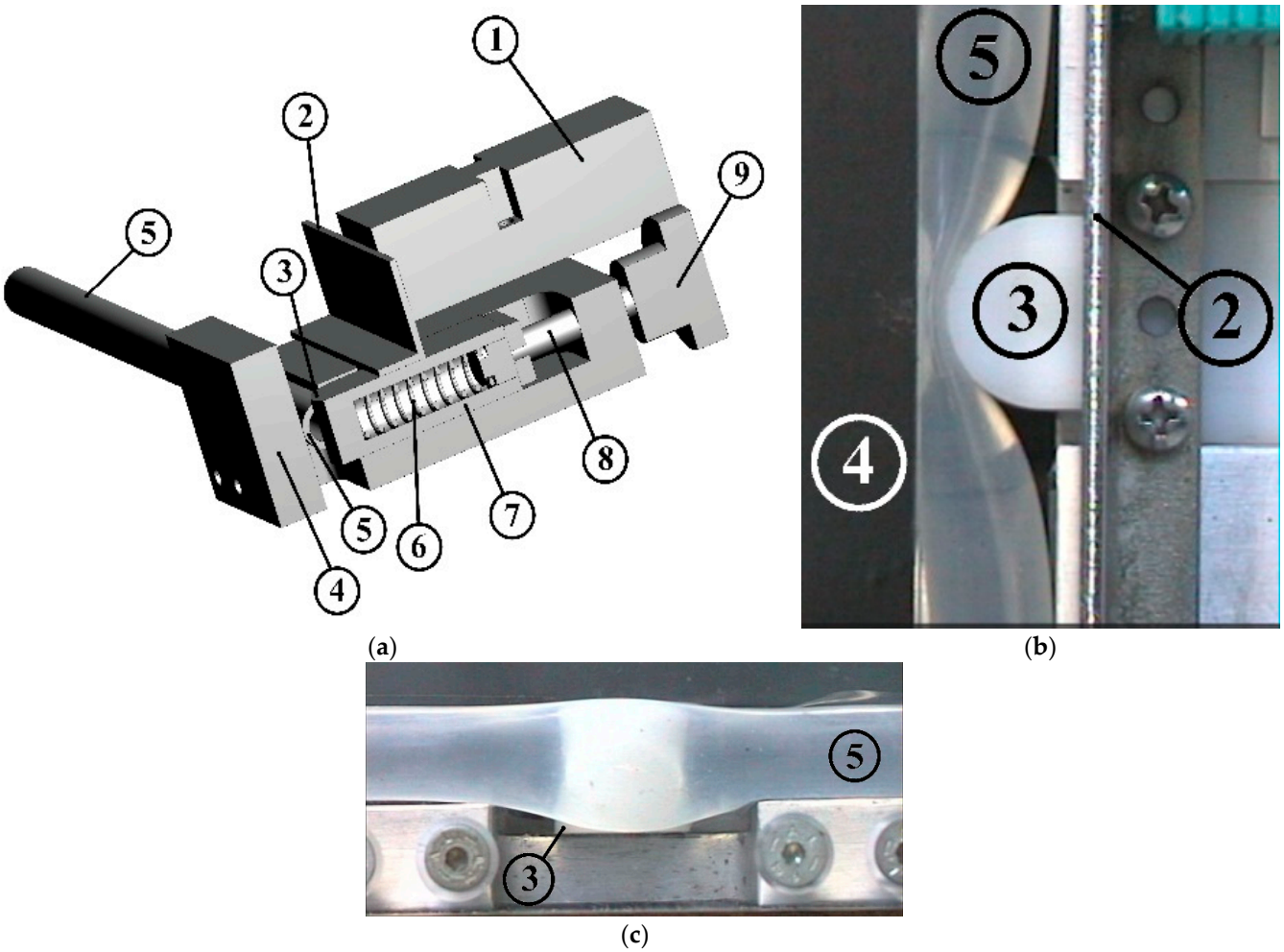

Figure 2. Stenosis device (from [12]). (**a**) Three-dimensional drawing: (1) inductive sensor for distance measurement; (2) metallic plate attached to the oscillating half-cylindrical piece; (3) half-cylindrical piece of Ertalon; (4) stationary plexiglas plate; (5) flexible tube; (6) compression spring; (7) spring case; (8) regulating screw; (9) screw handle meter. (**b**,**c**) Details of the half-cylindrical piece compressing the tube: (**b**) seen from above; (**c**) seen from the side.

The pincher, 100 mm long (L_1 = 100 mm), was asymmetrically located at a distance L_E = 220 mm from the flexible–stiff tube connection, and the oscillating stenosis was located at a distance of L_B = 180 mm, far from the center of the pincher (Figure 1). The frequency of the reciprocating pincher and the tube compression ratio $A_b = 1 - A_{min}/A_0$ (where A_{min} is the smallest tube cross-sectional area under the pincher, and A_0 is the undeformed flexible tube cross-sectional area) were both adjustable (see [12]). For each pinching frequency, the spring tension of the stenosis device was adjusted via a trial-and-error procedure in order to maximize the net flow rate. Setting the pump in operation, with the two water tanks having initially the same free surface elevation, with depths smaller than their maximum, an elevation difference progressively appeared between the tanks as time passed, accompanied by a reduction in the flow rate. Eventually, the flow rate was nullified, and the free surface height difference reached a maximum, depending on the pinching frequency and whether the stenosis was present or not. Therefore, a maximum flow rate was recorded when both tanks had the same free surface elevation. This is a typical characteristic feature of a valveless pump when it is connected to two tanks, as has been previously documented [11,13–15]. Thus, we decided to conduct all the experiments having filled the two tanks as shown in Figure 1b so that the free surface remained constant (not dependent on time), being identical for all the examined cases,

and at the same time, the net flow rate was the maximum one. As a result, the latter conditions facilitated comparisons of the valveless pumping performance with and without the presence of the proposed stenosis device in the present loop configuration. Moreover, the examined pinching frequencies (5.5 Hz to 11 Hz) and compression ratios (38%, 49%, 65%) were the same as in [12] (besides an additional compression ratio of 24%, which was also examined in this work), allowing for comparisons with the previous horizontal closed loop data.

The quantities which were examined as a function of time were as follows: (a) the time-dependent flow rate, which was measured by an electromagnetic flow meter (Carolina Medical FM501, Cary, NC, USA) connected to one of the two solid tubes of the hydraulic loop; (b) the gauge static pressures at the two solid–flexible tube junctions measured by piezoresistive transducers (MILLAR, Houston, TX, USA, SPC-370); (c) the displacement of the pincher via a wire sensor (Micro-Epsilon, Ortenburg, Germany); (d) the width of the unsteady stenosis neck via an inductive sensor (IA8-MIK-13, Pepperl + Fuchs, Mannheim, Germany); and (e) the gauge static pressure along the flexible tube via a piezoresistive transducer (MILLAR, Houston, TX, USA, SPC-370). The output analogue signals of the above sensors were digitized with a sampling frequency of 600 Hz and a minimum integration time of 20 s, employing 24-bit A/D converters (MX440A, HBM, Darmstadt, Germany) and 16-bit A/D converters (SPIDER8, HBM, Darmstadt, Germany) connected to two PCs. The synchronization of the two acquisition systems was based on a photodiode from which a voltage pulse was sent to both systems at an arbitrary time instant by inserting a metallic object between the two terminals of the photodiode (normally 30 s after the initiation of each experiment to avoid any transitional phenomena). The voltage pulse initiated the digitization of all signals exactly at the same time, which was the starting point of each experiment.

The uncertainty in the measured quantities in this work, for a confidence level of 95%, was as follows: flow rate: $\pm$1.6%; pressure: $\pm$3.3%; stenosis width: $\pm$3.8%; pincher displacement: $\pm$2.1%.

3. Results

All experiments were conducted with the free surface of the water tank maintained at 800 mm above the pincher of the valveless pump so that the maximum static gauge pressure in the loop was 800 mm H_2O or 58.86 mm Hg when the fluid was still. Note that the initial pressure in the horizontal loop of [12] (when the fluid was still) was 50 mmHg. It must also be noted that representative measurements were also made for a level of 1100 mm of the water tank (80.93 mmHg) without noticeable influence on the flow rate when the stenosis was used; whereas when the stenosis was absent, the flow rate was practically zero. On the other hand, smaller pressures than 50 mmHg in the loop did not allow the stenosis to oscillate due to the higher force applied externally by the spring device compared with the fluid pressure, so the performance of the proposed device was poor at low transmural pressures.

The net flow rate versus pinching frequency is shown in Figure 3 for three compression ratios—24%, 38%, and 49%—when the stenosis is present. The direction of the time mean flow is from the pincher towards the stenosis, with practically the same peak net flow rate values for A_b = 38% and 49%. In case in which the stenosis was not present, the flow rate was very small for the above compression ratios and of the opposite sign, taking mean values 0.03 L/min for A_b = 24% and 0.12 L/min for A_b = 38% and 49%. In contrast, when the stenosis was present, the peak flow rates were 0.57 L/min, namely, 19 times larger for A_b = 24% and 0.76 L/min (or 6.3 times larger) for A_b = 38% and 49%. It is clear that without the stenosis, the valveless pump was not operable in the present configuration for small compression ratios, verifying the value of the proposed device for boosting the flow rate. The major difference from the horizontal loop of [12] is that the flow rates in the present loop were about 50% smaller, whether the stenosis was present or not. Peaks and valleys did appear in the net flow rate versus pinching frequency graph, the latter being

less smooth compared with the horizontal loop case. Therefore, it seems that gravity plays an important role in valveless pumping, a parameter which has been highlighted by [13]. Moreover, the presence of the open tank, with its free surface being constant, caused the pressure at this location of the hydraulic loop to be time-invariant, independently of the pinching frequency, the compression ratio, and the presence or absence of the stenosis. Although the net flow rate is expected to increase with the pinching frequency due to the larger displaced fluid volume by the pincher per unit of time, this does not happen because of the complex interaction of the fluid with the flexible tube walls. As a result, multiple peaks normally appear in the flow rate versus frequency curves of the valveless pumps, as well as flow direction reversals. The flow rate peaks has been shown by many researchers, as well as by our group [2,3], to be related to the resonance phenomenon.

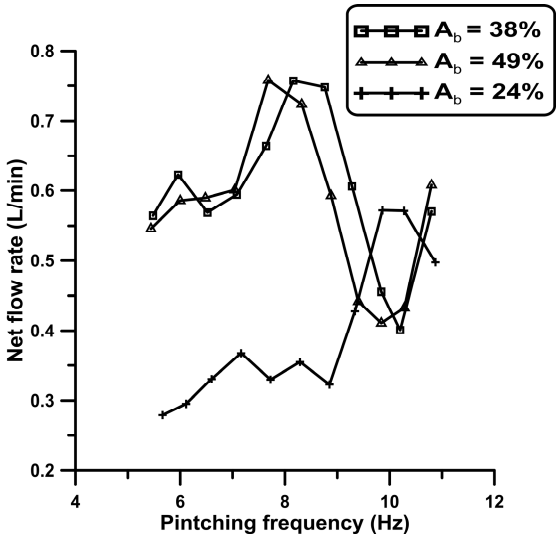

Figure 3. Net flow rate versus pinching frequency with the stenosis present for three compression ratios A_b: 24%, 38%, and 49%.

When the compression ratio was increased to 65%, the influence of the stenosis on the flow rate was weakened (like in [12]), as shown in Figure 4, with the flow rates being comparable between the two cases. The flow direction for A_b = 65% was the opposite between the stenosis and the non-stenosis case for pinching frequencies smaller than f = 9.85 Hz, which also occurred for smaller A_b values. However, for higher pinching frequencies, the flow direction was reversed for the non-stenosis case, a typical behavior of valveless pumping wherein the flow is nullified (coinciding with a change in flow direction) at multiple frequencies. It must be remembered that at low pinching frequencies (below the first resonance frequency), the flow direction (in the case where the stenosis is absent) is from the pincher to the closer tube junction, as has been evidenced by many researchers [14,15], including our group [3,16]. Since the stenosis was installed in this work at the longer part of the flexible tube, an opposite flow was established between the two cases (stenosis versus no-stenosis) for f > 9.85 Hz.

The behavior of a valveless pump is quite complex for two main reasons: (a) the interaction of the fluid with the deformable tube walls; and (b) the presence of the flexible–rigid tube junctions. During the tube compression phase by the pincher, the pressure increases due to the tube dilation in the rest of the flexible tube, which is a function of the tube's material properties (Young's modulus, Poisson's ratio) and the tube's geometrical features (tube inner radius and wall thickness) (see [12]). Thus, pressure waves are generated at the pincher area and travel along the flexible tube with a finite speed, reflected at the tube junctions. Consequently, the axial pressure distribution is affected accordingly, which, in turn, affects the tube shape and the flow rate. In the present work, a deformable stenosis is introduced at a small distance from the pincher, the shape of which varies in time due

to the time-dependent pressure and the opposing force of a spring. In Figure 5, three quantities are shown for each compression ratio versus the non-dimensional time t/T (T is the pinching period)—namely, (a) the pincher displacement in cm; (b) the opening of the stenosis neck in mm; and (c) the flow rate in L/min—for 5.96 Hz and for the frequency of the maximum flow rate of each case. The common feature of the curves shown in Figure 5 is that during the compression phase (wherein the displacement of the pincher is shown to be reduced in the graphs), the stenosis opening increases as well as the flow rate, as recorded in one of the stiff tubes of the loop. In contrast, during decompression, the stenosis neck width is reduced (due to the reduced pressures), restricting the backflow towards the pincher, thus enhancing the unidirectional flow from the pincher to the stenosis. The flow rate was maximized a little before the end of the compression phase, with an amplitude which did not exceed 20% of the net flow rate and 10% of the peak net flow rates. Similar behavior was observed for A_b = 65% for the no-stenosis case (Figure 5g,h). It has to be noted that in the subsequent graphs, in order to improve their clarity, the symbols shown are much fewer than the actual measured points.

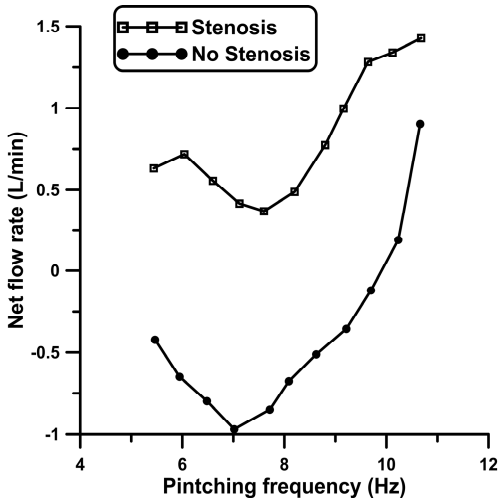

Figure 4. Net flow rate versus pinching frequency for A_b = 65%.

It is noteworthy that the stenosis neck maximum width was of the order of 2 mm or 16% of the tube diameter, whereas its minimum was zero (or slightly negative in some cases), corresponding to a deep occluded case. The stenosis opening was dependent on the spring tension and the opposing pressure force, the first being adjusted by a trial-and-error procedure, aiming at flow rate maximization. It is important to note that as was shown in [12], small spring pretension, which allows for large openings of the stenosis, or high spring pretention, which hinders the oscillatory motion of the stenosis, do not augment the flow rate; that is, the flow rate is affected by the stenosis only if its opening is time-dependent, and, compared to the tube diameter, it varies within a certain small interval.

As mentioned above, the pressure wave reflections at the flexible–rigid tube junctions play a major role in valveless pumping. The consequence of the latter is the variation of the pressure amplitude along the tube, which was documented here by inserting a pressure catheter at the tube junction and moving it inside the flexible tube to various cross-sections. A representative variation of the peak-to-peak pressure amplitude along the flexible tube is shown in Figure 6 for A_b = 38% and a pinching frequency 8.16 Hz, with the distance measured from the stenosis neck. The curve with the higher values corresponds to the no-stenosis case.

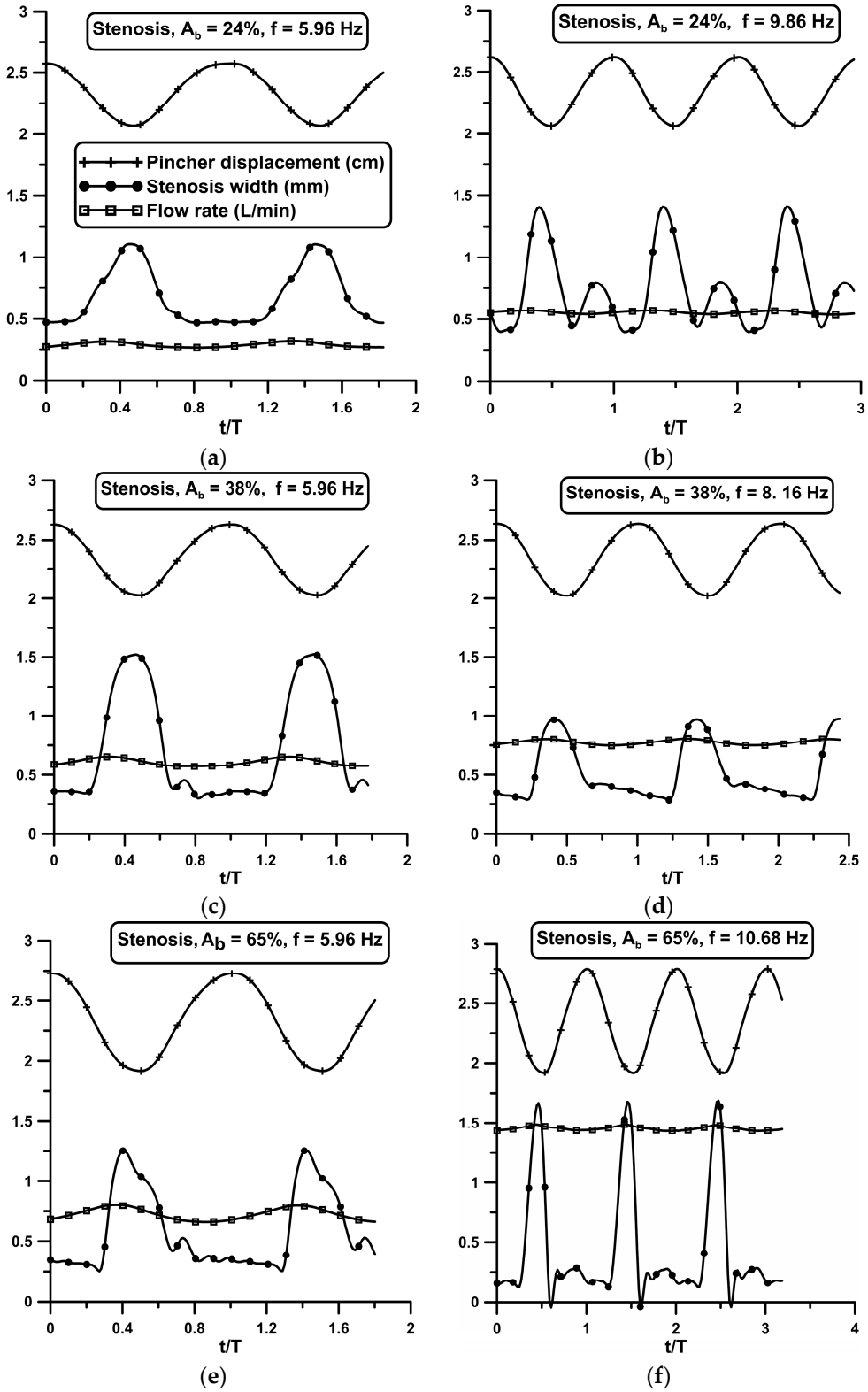

Figure 5. *Cont.*

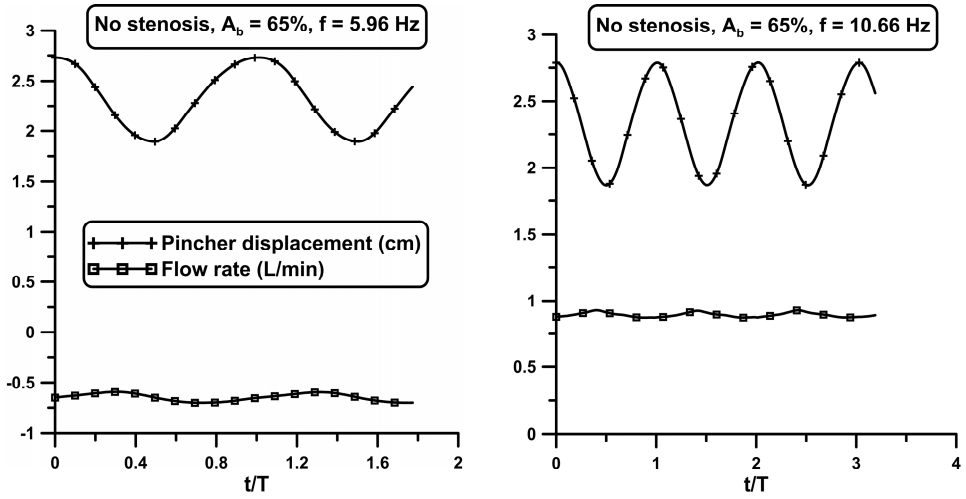

Figure 5. Time series of pincher displacement, stenosis width, and flow rate. Explanations for the symbols are given in (**a**). (**a**–**f**) Stenosis is present: (**a**) A_b = 24%, f = 5.96 Hz; (**b**) A_b = 24%, f = 9.86 Hz; (**c**) A_b = 38%, f = 5.96 Hz; (**d**) A_b = 38%, f = 8.16 Hz; (**e**) A_b = 65%, f = 5.96 Hz; (**f**) A_b = 65%, f = 10.68 Hz. (**g**,**h**) No stenosis is presents: (**g**) A_b = 65%, f = 5.96 Hz; (**h**) A_b = 65%, f = 10.66 Hz.

According to [17] (Equation (8.7.27)), the pressure amplitude p^* along a flexible tube connected with a tube of different compliance, non-dimenionalized by the pressure amplitude at the entrance of the tube (where a harmonic pressure variation is generated), is given by the following formula:

$$p^*(\bar{x}) = \sqrt{1 + R^2 + 2Rcos(\frac{4\pi}{\bar{\lambda}}(\bar{x} - 1))}, \tag{1}$$

where R is the reflection coefficient, $\bar{\lambda} = \lambda/L$ is the non-dimensional wavelength (λ) of the generated pressure waves, and $\bar{x} = x/L$ is the non-dimensional distance (x) from the tube entrance, both non-dimensionalized by the length of the tube L. The reflection coefficient at the junction of two tubes, say tube 1 and tube 2 of equal diameters and wave speeds c_1 and c_2, is ([17], Equations (9.5.11) and (9.5.17))

$$R = \frac{c_2 - c_1}{c_2 + c_1} = \frac{1 - c_1/c_2}{1 + c_1/c_2} \tag{2}$$

when the flow direction is from tube 1 to tube 2. The wave speed (see [12]) is

$$c = \sqrt{\frac{Et}{\rho D(1 - \sigma^2)}}, \tag{3}$$

where ρ is the fluid density, t is the tube thickness, D is the internal tube diameter, σ is the tube material's Poisson's ratio, and E its Young's modulus. Since the Young's modulus of the stiff tube was many orders of magnitude larger compared with that of the flexible tube, namely, 1400 MPa compared to 2.38 MPa of the flexible tube (see [3,12]), the ratio of the wave speeds was

$$c_1/c_2 \sim \sqrt{E_1/E_2} = 0.04 \tag{4}$$

and $R \sim 0.923$.

According to Equation (1), the pressure amplitude p^* is an increasing function of x if $\bar{\lambda} \geq 4$; otherwise, it exhibits a minimum, which is not related to the case presented in Figure 6. Based on Equation (1), the distribution of p^* along the tube is shown in Figure 7 for three values of $\bar{\lambda}$, namely, 3, 4, and 5.

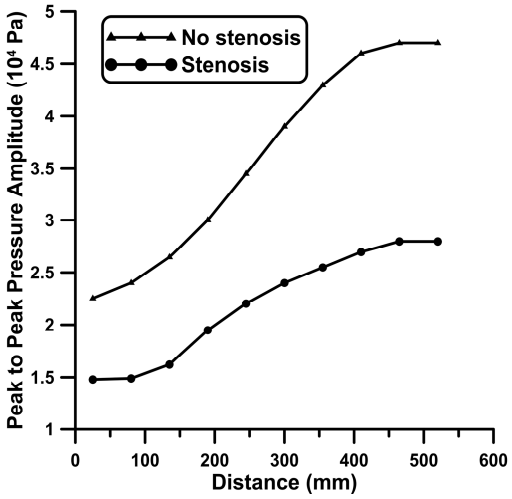

Figure 6. Peak-to-peak pressure amplitude along the flexible tube with the stenosis and without the stenosis: A_b = 38%, f = 8.16 Hz.

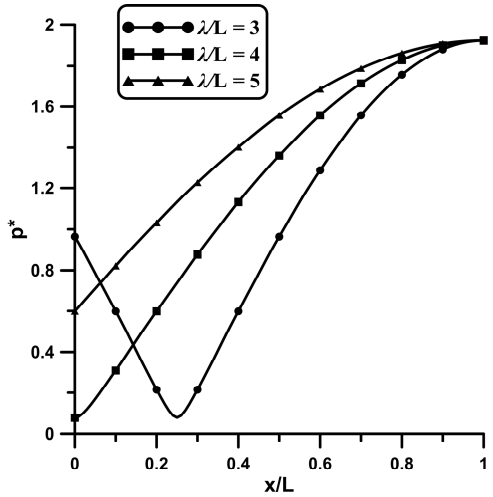

Figure 7. Pressure amplitude streamwise distribution according to Equation (1) for λ/L = 3, 4, and 5 and for R = 0.923.

Assuming that the flexible tube starts at the end of the pincher, which plays the role of a pressure wave generator, the closest pressure measurement was 155 mm from it, or $\overline{x}$ = 0.24, based on the tube length from the pincher to the tube junction, which was L = 650 mm. According to Figure 6, the ratio of the pressure amplitudes at the tube end ($\overline{x}$ = 1) to that at $\overline{x}$ = 0.24 is 2.09 for the no-stenosis case. Therefore, using $\overline{x}$ = 0.24 in Equation (1), and knowing that the pressure amplitude at $\overline{x}$ = 1 is R + 1 (see [17], Equation (8. 7.30)), the value of $\overline{\lambda}$ that satisfies the above pressure ratio of 2.09 is 4.45. Therefore, the wavelength, λ, of the pressure waves was 4.45 × 650 = 2890 mm for a pinching frequency f = 8.16 Hz. As a result, the wave speed was c_1 = λf = 2.89 × 8.16 = 23.58 m/s. It is interesting to note that in [12], the wave speed was estimated to be 15.6 m/s, or 33.8% smaller, based on two assumptions: the fluid was stationary, and the gauge pressure was zero. However, when the flow is pulsating, pressure takes on mean values higher than zero and the tube becomes stiffer, causing an increase in the tube's Young's modulus and, consequently, an increase in the wave speed. The pressure measurements for a lower pinching frequency of 5.44 Hz and A_b = 38% showed similar trends, albeit with smaller variations along the tube, which are attributed to the larger wavelength $\lambda = c_1/\mathrm{f}$ = 23.58/5.44 = 4.33 m (see Figure 7).

The presence of the stenosis reduced the pressure amplitude for A_b = 38%, according to Figure 6, while its variation along the tube was similar to that without the stenosis. In Figure 8, representative pressure waveforms are shown at three cross-sections along the tube for f = 8.16 Hz and A_b = 38%, with and without the stenosis, namely, at 2.08 D, 20.41 D, and 43.3 D from the stenosis neck, respectively. The last station (x = 43.3 D) coincides with the flexible–rigid tube junction. During the compression phase, the pressure increased sharply, with an increasing phase lag along the tube, which was maximized at the tube junction at about T/4. A consequence of the phase lag is that the axial pressure gradient changed sign in each period, being negative during compression and before the pressure peak, turning positive around the pressure peak, and becoming again negative during decompression. It is also interesting to note that during compression, the pressure at the closest distance from the stenosis neck exhibits two peaks and a local minimum. A probable explanation of such variation is that when compression starts, the pressure increases (due to tube dilation), but since the stenosis opens simultaneously, the flow accelerates, causing a local pressure reduction. In the next time steps that the stenosis tends to close, the flow speed is reduced, and the pressure increases again.

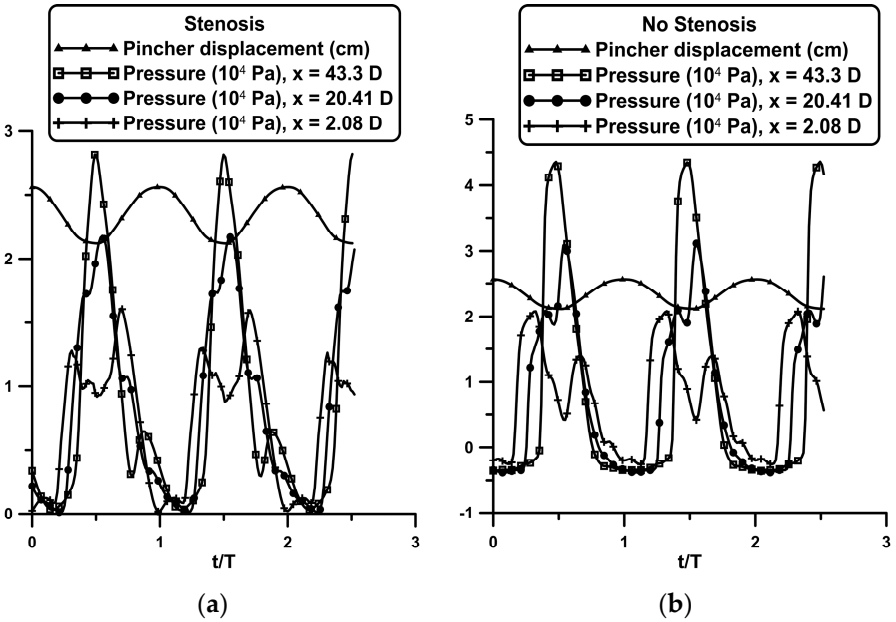

Figure 8. Pincher displacement and peak-to-peak pressure amplitudes along the flexible tube at three distances from the stenosis neck: 2.08 D, 20.41 D, and 43.3 D for A_b = 38%, f = 8.16 Hz. (**a**) Stenosis; (**b**) no-stenosis.

Phase difference was also detected, as expected, between the pressure waveforms at the two flexible–rigid tube junctions, the farthest presenting a phase lag between 0.2 T and 0.25 T or 72° and 90°, as is documented in Figure 9. The latter phase angles can be explained based on (a) the lengths of the flexible tube between the pincher and the tube junctions, namely, 650 mm and 170 mm, respectively; and (b) the wave speed of 23.58 m/s. If the wave speed is assumed to be independent of the pinching frequency, the time difference between the two waves traveling from the pincher to the tube junctions for the lowest pinching frequency (f = 5.66 Hz) is 0.152 T = 54°, and for the maximum frequency (f = 10.8 Hz), it is 0.22 T = 79.2°.

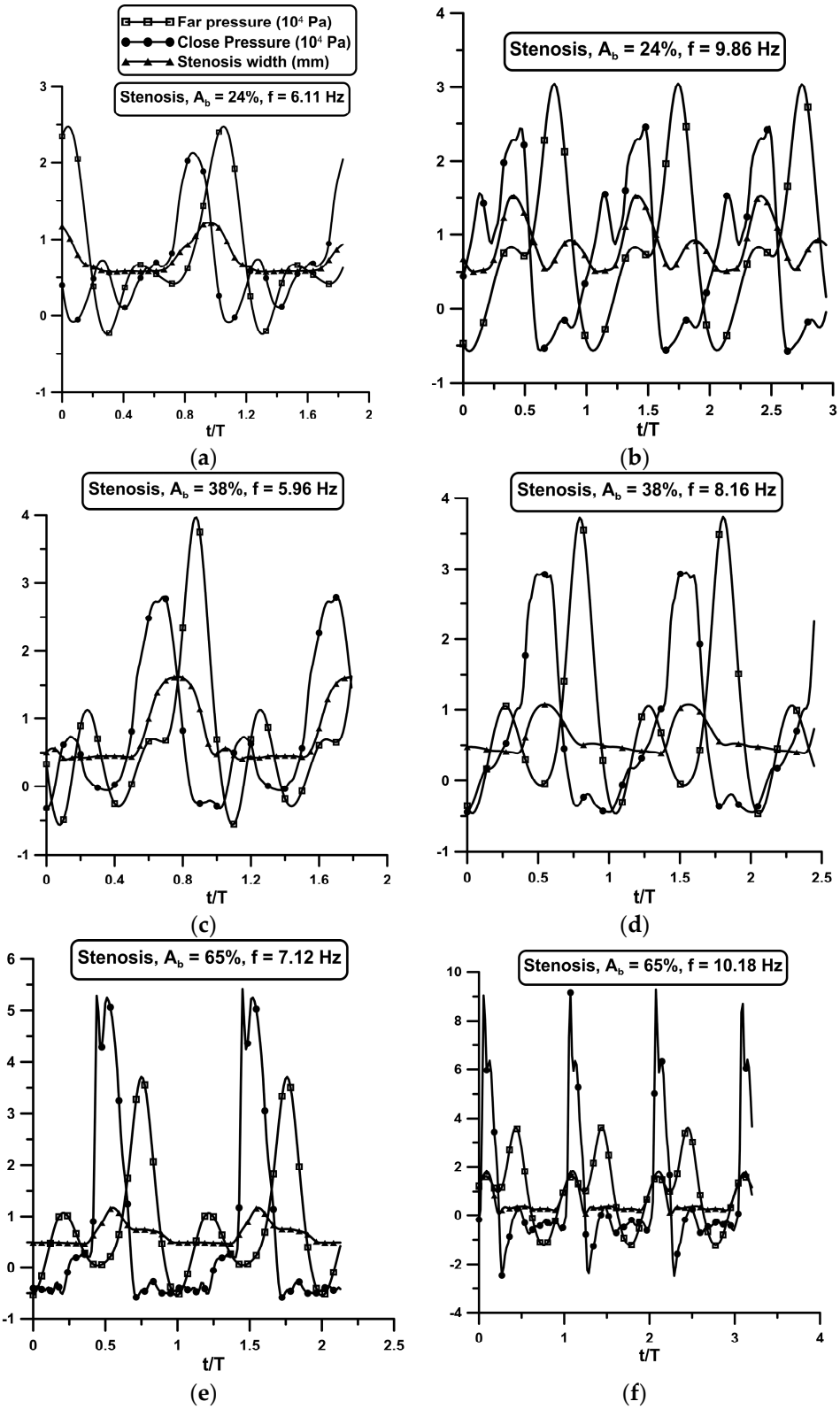

Figure 9. *Cont.*

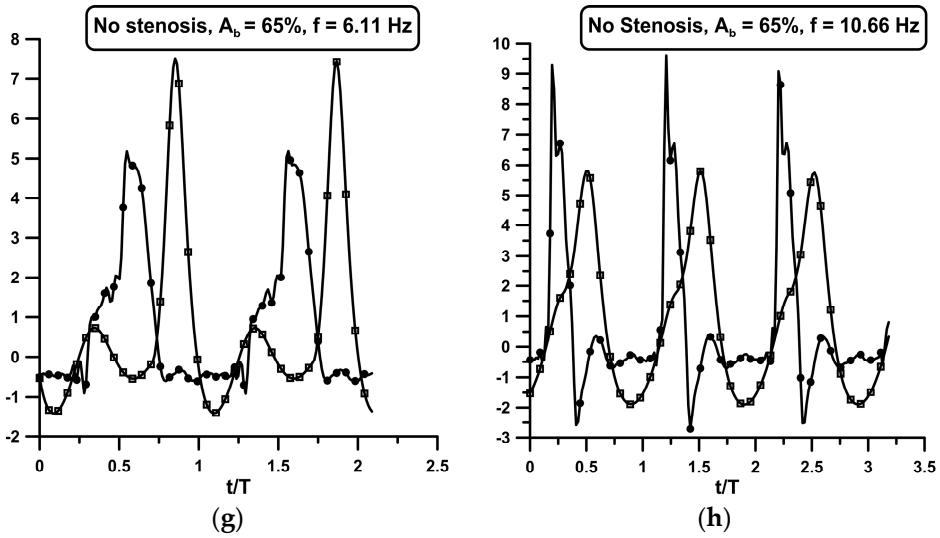

Figure 9. Pressure time series at the two flexible–rigid tube junctions (far and close) and stenosis width. Symbols explanations are given in (**a**). (**a**–**f**) Stenosis is present: (**a**) A_b = 24%, f = 6.11 Hz; (**b**) A_b = 24%, f = 9.86 Hz; (**c**) A_b = 38%, f = 5.96 Hz; (**d**) A_b = 38%, f = 8.16 Hz; (**e**) A_b = 65%, f = 7.12 Hz; (**f**) A_b = 65%, f = 10.18 Hz. (**g**,**h**) No stenosis is present: (**g**) A_b = 65%, f = 6.11 Hz; (**h**) A_b = 65%, f = 10.66 Hz.

The extreme pressure values at the two junctions are presented in Figures 10 and 11, taking positive gauge values up to 100 kPa and negative down to −30 kPa. In general, the pressure amplitudes increase with the pinching frequency (mainly related to the increased fluid inertia) and the compression ratio, which is related to higher flow rates.

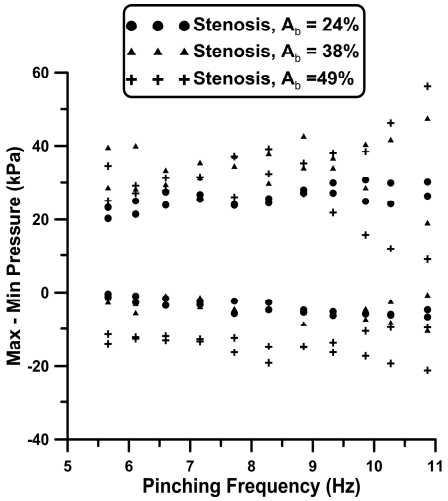

Figure 10. Extreme pressure values with stenosis present: A_b = 24%, 38%, and 48%.

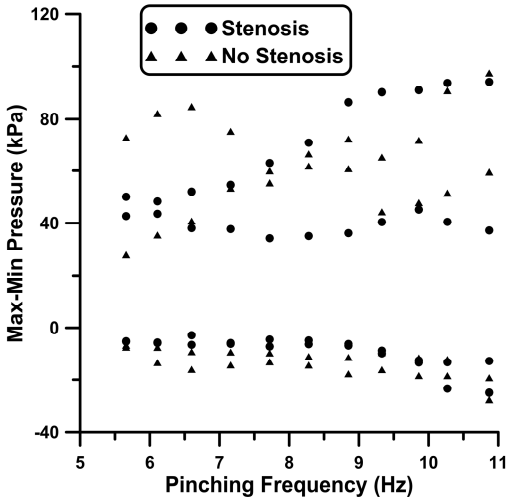

Figure 11. Extreme pressure values for A_b = 65% for stenosis and no-stenosis cases.

4. Discussion

The objective of the present work was to examine the influence of the unsteady stenosis in valveless pumping, taking into account gravity, which was practically absent in the horizontal loop of our previous work. Initially, the experiments were conducted using two tanks with the same free surface height, which changed as time progressed due to pumping, and at the same time, the flow rate was reduced. Eventually, the flow rate became null, and a height difference was established between the two tanks, which was dependent on the pinching frequency and the presence or not of the stenosis. Seeking the maximum possible flow rates of the valveless pump, it was decided to replace the two tanks with one, the height of which was always constant at 800 mm. Since the area of the free surface of the tank was 500 cm^2 and the maximum volume of the fluid displaced by the pincher was only 11.3 cm^3, the free surface height was practically constant, as was the static pressure at the joints of the two rigid tubes of the loop, equal to 150 mm = 1.47 kPa. The average static pressures at the flexible–rigid tube junctions were about 10 kPa, which dropped to the latter value of 1.47 kPa mainly due to gravity (800 mm = 7.84 kPa). Regarding the hydraulic losses, at the entrance of the tank, these were equal to the fluid kinetic energy; that is, for a maximum examined flow rate of 1.5 L/min, they were 24 Pa, and the linear losses are estimated to be 63 Pa based on the mean bulked fluid speed and Darcy's formula, assuming laminar flow (Re = 2640). It has to be noted that according to [18], Darcy's formula is valid for pulsating tube flows, whether the flow is laminar or turbulent.

It is interesting to note that the pressure amplitudes along the flexible tube when the stenosis was present were significantly reduced compared to the non-stenosis case. For A_b = 38% and a pinching frequency f = 8.16 Hz, the amplitude ratios (stenosis to no-stenosis cases) varied from 57% to 68% along the tube, despite the six-times-larger net flow rates of the stenosis case. The same trend was observed for the same A_b and a smaller frequency (f = 5.48 Hz), although the ratios were larger, varying from 65% to 75%. The latter indicates that at low pinching frequencies, the stenosis' influence on the pressure amplitude attenuation is smaller. Conclusively, the unsteady stenosis caused not only an increase in the net flow rate but also a reduction in the pressure pulsations. It has to be noted that the vibrations of the flexible tube walls were notably reduced when the stenosis was present. A reduction in the pressure pulsations due to a stenosis in a flexible tube has also been observed in [19], attributed to the stenosis hydraulic losses. Conclusively, pressure amplitudes are irrelevant to net flow rates since these are related predominantly to fluid acceleration–deceleration and the compliance of the flexible tube.

The pressure time variation at the tube junctions is characterized as more or less sinusoidal, combined with oscillations of decaying amplitude; that is, during tube compression, the pressure increased, and during decompression, it decreased, followed by damped oscil-

lations as it occurs in a free vibrating system after its initial excitation (Figure 9). The same behavior was recorded in [3] (Figure 7) and in [20] (Figure 3), in which, at small pinching frequencies, compared to the natural frequency of the hydraulic loop, there were multiple pressure oscillations of small amplitude within each pinching period, superimposed on the basic oscillation imposed by the pincher.

The flow rate amplitudes were not affected by the presence of the stenosis. Moreover, at the lowest pinching frequency, the flow rate pulsations were normally up to 20% of the time mean value, whereas at high frequencies, the amplitudes were reduced so that they did not exceed 10% of the mean.

Regarding the volumetric efficiency of the pump, when the stenosis was present, it varied from 38% to 32% for A_b = 24% to 65%; whereas without the stenosis, it changed from 2% to 20%, exhibiting the stenosis' significant role in flow augmentation. On the other hand, in the horizontal loop of [12], the volumetric efficiency was much higher, namely, when the stenosis was present, it dropped from 77% to 50% for A_b = 38% to 65%, and without the stenosis it increased from 11% to 37%.

It is important to mention that the experiments were conducted by adjusting, for each pinching frequency, the pretension of the spring by rotating the regulating screw of the stenosis device by a few degrees, aiming at maximization of the flow rate. An improvement of the procedure and the efficiency of the stenosis would be achieved using a controllable motor, which would rotate the regulating screw of the spring device at small steps, using the flow rate as a feed-back control signal.

A final note regarding the reduced influence of the stenosis with increasing compression ratios: a probable explanation might be the increased hydraulic losses at the pincher due to the high compression ratio, so when these are combined with the losses of the stenosis, the total available input energy cannot be transformed to increased flow rates; therefore, the proposed device's limitation is that its influence on flow rate augmentation is only significant for compression ratios lower than 50%.

5. Conclusions

The beneficial role of an unsteady stenosis in increasing the net flow rate in valveless pumping was experimentally examined. The pump was connected to a loop, including an open water tank at a height of 800 mm above the pump's pincher, in contrast to a horizontal loop, which was examined by the same group in a previous study. The presence of the stenosis increased the flow rates by up to 19 times for a compression ratio A_b = 24% and 6.5 times for A_b = 38% and 48%; whereas for A_b = 65%, its influence was minimal. The increase in the net flow rate is attributed to the opening and closing of the stenosis in such a way that the fluid mass within each pinching period is directed more from the pincher to the stenosis than backwards; that is, the stenosis opened during the compression phase of the pincher due to the elevated pressures, which varied from 20 kPa to 100 kPa, and closed during decompression such that the gauge pressures took on negative values down to −30 kPa, thus restricting the backward flow. The pressure increase at the stenosis area during compression is attributed to the flexible tube dilation due to the fluid mass expelled by the pincher, the inertial forces related to fluid acceleration, the gravitational force of the vertical fluid column, and the reflected pressure waves at the tube junctions. Evidence of the pressure reflections includes the recorded increase in the pressure amplitude along the tube from the stenosis to the tube junction, which was strongly attenuated by the presence of the stenosis, especially at higher pinching frequencies. An improvement to the proposed spring device would be based on a programmable motor which would change the pretension of the spring based on the flow rate signal.

Author Contributions: Conceptualization, D.M.; methodology, D.M. and C.M.; software, D.M.; validation, C.M. and D.M.; formal analysis, D.M. and C.M.; investigation, C.M. and D.M.; data curation, D.M. and C.M.; writing—original draft preparation, D.M. and C.M.; writing—review and editing, D.M. and C.M.; visualization, D.M. and C.M. All authors have read and agreed to the published version of the manuscript.

Funding: This research received no external funding.

Data Availability Statement: The raw data supporting the conclusions of this article will be made available by the authors on request.

Conflicts of Interest: The authors declare no conflicts of interest.

References

1. Ozanam, M. De la circulation veineuse par influence. *Comptes Rendus Hebd. Seances Acad. Sci.* **1881**, *93*, 92–94.
2. Hickerson, A.I.; Gharib, M. On the resonance of a pliant tube as a mechanism for valveless pumping. *J. Fluid Mech.* **2006**, *555*, 141–148. [CrossRef]
3. Manopoulos, C.; Tsangaris, S.; Mathioulakis, D. Net flow generation in closed-loop valveless pumping. *Proc. Inst. Mech. Eng. Part C J. Mech. Eng. Sci.* **2020**, *234*, 2126–2142. [CrossRef]
4. Yan, Q.; Yin, Y.; Sun, W.; Fu, J. Advances in Valveless Piezoelectric Pumps. *Appl. Sci.* **2021**, *11*, 7061. [CrossRef]
5. Khabarova, D.F.; Podzerko, A.V.; Spiridonov, E.K. Experimental Investigation of Fluidic Diodes. *Procedia Eng.* **2017**, *206*, 93–98. [CrossRef]
6. Bohm, S.; Hai, B.P.; Moriyama, A.; Runge, E.; Strehle, S.; König, J.; Cierpka, C.; Dittrich, L. Highly efficient passive Tesla valves for micro fluidic applications. *Microsyst. Nanoeng.* **2022**, *8*, 97. [CrossRef] [PubMed]
7. Nguyen, Q.M.; Abouezzi1, J.; Ristroph, L. Early turbulence and pulsatile flows enhance diodicity of Tesla's macro fluidic valve. *Nat. Commun.* **2021**, *12*, 2884. [CrossRef] [PubMed]
8. Laser, D.J.; Santiago, J.G. A review of micropumps. *J. Micromech. Microeng.* **2004**, *14*, 35–64. [CrossRef]
9. Hou, Y.; He, L.; Hu, D.; Zhang, L.; Yu, B.; Cheng, G. Recent trends in structures and applications of valveless piezoelectric pump—A review. *J. Micromech. Microeng.* **2022**, *32*, 053002. [CrossRef]
10. Amselem, G.; Clanet, C.; Benzaquen, M. Valveless pumping at low Reynolds numbers. *Phys. Rev. Appl.* **2023**, *19*, 024017. [CrossRef]
11. Anatol, J.; García-Díaz, M.; Barrios-Collado, C.; Moneo-Fernández, J.; Castro-Ruiz, F.; Sierra-Pallares, J. Experimental characterization of an asymmetric valveless pump based on soft robotics technology. *Phys. Fluids* **2023**, *35*, 061904. [CrossRef]
12. Manopoulos, C.; Mathioulakis, D. Flow Rate Augmentation of Valveless Pumping via a Time-Dependent Stenosis: A Novel Device. *Fluids* **2023**, *8*, 249. [CrossRef]
13. Timmermann, S.; Ottesen, J.T. Novel characteristics of valveless pumping. *Phys. Fluids* **2009**, *21*, 053601. [CrossRef]
14. Bredow, H. *Untersuchung Eines Ventillosen Pumpprinzips*; VDI-Verlag: Düsseldorf, Germany, 1968; Volume 7, pp. 1–89. Available online: https://www.tib.eu/en/search/id/TIBKAT:196829372 (accessed on 4 February 2024).
15. Mahrenholtz, O.; Bredow, H.J. Modelle ventilloser Pumpen. In *Phänomen der Pulsierenden Strömung im Blutkreislauf aus Technologischer, Physiologischer und Klinischer Sicht*; Pestel, E., Liebau, G., Eds.; Bibliographisches Institut: Wien, Austria, 1970; pp. 738/738a*79–87.
16. Manopoulos, C.; Mathioulakis, D.; Tsangaris, S. One-dimensional model of valveless pumping in a closed loop and a numerical solution. *Phys. Fluids* **2006**, *18*, 017106. [CrossRef]
17. Zamir, M. *The Physics of Coronary Blood Flow*; Springer: London, ON, Canada, 2005.
18. Shemer, L.; Wygnanski, I.; Kit, E. Pulsating flow in a pipe. *Fluid Mech.* **1985**, *153*, 313–337. [CrossRef]
19. Kumar, K.; Prabhakaran, D. Dynamics of a collapsible tube with internal constriction. *Phys. Fluids* **2022**, *34*, 121905. [CrossRef]
20. Bringley, T.; Childress, S.; Vandenberghe, N.; Zhang, J. An experimental investigation and a simple model of a valveless pump. *Phys. Fluids* **2008**, *20*, 033602. [CrossRef]